



**Role of coexisting tetragonal regions in the rhombohedral phase of Na<sub>0.5</sub>Bi<sub>0.5</sub>TiO<sub>3</sub>-xat.%BaTiO<sub>3</sub> crystals on enhanced piezoelectric properties on approaching the morphotropic phase boundary**

Jianjun Yao, Niven Monsegue, Mitsuhiro Murayama, Weinan Leng, William T. Reynolds, Qinhui Zhang, Haosu Luo, Jiefang Li, Wenwei Ge, and D. Viehland

Citation: [Applied Physics Letters](#) **100**, 012901 (2012); doi: 10.1063/1.3673832

View online: <http://dx.doi.org/10.1063/1.3673832>

View Table of Contents: <http://scitation.aip.org/content/aip/journal/apl/100/1?ver=pdfcov>

Published by the [AIP Publishing](#)

---

Copyright by the American Institute of Physics (AIP). Yao, Jianjun; Monsegue, Niven; Murayama, Mitsuhiro; et al., "Role of coexisting tetragonal regions in the rhombohedral phase of Na<sub>0.5</sub>Bi<sub>0.5</sub>TiO<sub>3</sub>-xat.%BaTiO<sub>3</sub> crystals on enhanced piezoelectric properties on approaching the morphotropic phase boundary," Appl. Phys. Lett. 100, 012901 (2012); <http://dx.doi.org/10.1063/1.3673832>



## Re-register for Table of Content Alerts

Create a profile.



Sign up today!



# Role of coexisting tetragonal regions in the rhombohedral phase of $\text{Na}_{0.5}\text{Bi}_{0.5}\text{TiO}_3$ - $x\text{at.}\%\text{BaTiO}_3$ crystals on enhanced piezoelectric properties on approaching the morphotropic phase boundary

Jianjun Yao,<sup>1,a)</sup> Niven Monsegue,<sup>2</sup> Mitsuhiro Murayama,<sup>1,2</sup> Weinan Leng,<sup>2</sup> William T. Reynolds,<sup>1</sup> Qinhui Zhang,<sup>3</sup> Haosu Luo,<sup>3</sup> Jiefang Li,<sup>1</sup> Wenwei Ge,<sup>1</sup> and D. Viehland<sup>1</sup>

<sup>1</sup>Department of Materials Science and Engineering, Virginia Tech, Blacksburg, Virginia 24061, USA

<sup>2</sup>Institute for Critical Technology and Applied Science, Virginia Tech, Blacksburg, Virginia 24061, USA

<sup>3</sup>Shanghai Institute of Ceramics, Chinese Academy of Sciences, 215 Chengbei Road, Jiading, Shanghai 201800, China

(Received 17 September 2011; accepted 10 December 2011; published online 3 January 2012)

The ferroelectric domain and local structures of  $\text{Na}_{0.5}\text{Bi}_{0.5}\text{TiO}_3$ - $x\text{at.}\%\text{BaTiO}_3$  (NBT- $x\%$ BT) crystals for  $x = 0, 4.5,$  and  $5.5$  have been investigated by transmission electron microscopy. The results show that the size of polar nano-regions was refined with increasing  $x\text{at.}\%\text{BT}$ . The tetragonal phase volume fraction, as identified by in-phase octahedral tilting, was found to be increased with BT. The findings indicate that the large electric field induced strains in morphotropic phase boundary compositions of NBT- $x\%$ BT originate not only from polarization rotation but also polarization extension. © 2012 American Institute of Physics. [doi:10.1063/1.3673832]

Piezoelectric materials are widely used in actuators, sensors, and transducers. These commercially used piezoelectrics are based on lead zirconate titanate (or PZT) solid solutions, which have superior dielectric and piezoelectric properties.<sup>1</sup> Environmental concerns are presently driving the development of alternative lead-free piezoelectrics: the goal is bulk materials with comparable piezoelectric properties to PZT. Solid solutions of  $\text{Na}_{0.5}\text{Bi}_{0.5}\text{TiO}_3$ -based (NBT) perovskites are leading candidate lead-free ferroelectrics in these regards,<sup>2</sup> as high longitudinal piezoelectric constants of  $d_{33} \approx 500$  pC/N have been reported for NBT- $x\%$ BT single crystals with compositions close to a morphotropic phase boundary (MPB).<sup>3,4</sup> Such large piezoelectric constants and high electric field induced strains in this system offer promise for Pb-free sensors and actuators.<sup>5</sup>

Near the MPB of  $\text{Pb}(\text{Mg}_{1/3}\text{Nb}_{2/3})\text{O}_3$ - $x\%\text{PbTiO}_3$  (PMN- $x\%$ PT) and  $\text{Pb}(\text{Zn}_{1/3}\text{Nb}_{2/3})\text{O}_3$ - $x\%\text{PbTiO}_3$  (PZN- $x\%$ PT) crystals, structurally bridging monoclinic ( $M$ ) phases that separate rhombohedral ( $R$ ) and tetragonal ( $T$ ) ones have been reported.<sup>8,9</sup> Polarization rotation within these  $M$  phases is believed to be the mechanism of enhanced piezoelectricity. The MPB of NBT- $x\%$ BT is found near  $5.5 < x < 6.5$  at.%,<sup>2,6,7</sup> where the highest piezoelectric constants and electric field induced strains are found.<sup>3-5</sup> In spite of comprehensive investigations of NBT- $x\%$ BT, structurally bridging  $M$  phases have not been found that have significant  $c/a$  ratios in domain engineered states, similar to that of PMN-PT and PZN-PT.<sup>8,9</sup> However, recent evidence exists of a very weak monoclinicity for NBT, suggesting that it may not have a strong correlation between polarization rotation in a monoclinic distorted structure and enhanced piezoelectricity.<sup>10,11</sup> Thus, the mechanism of enhanced piezoelectricity in MPB compositions of NBT- $x\%$ BT remains in question. An alternative model of an electric field induced nonpolar (or pseu-

docubic) to ferroelectric transition was proposed to explain a giant strain observed near the MPB for NBT- $x\%$ BT.<sup>12-14</sup> To date, a detailed understanding of the local nonpolar structure is unclear, especially its evolution with compositions approaching the MPB. Therefore, systematic studies of the complex structural evolution with  $x$  would help to evaluate the structure-property relations and to identify the mechanism of enhancement near the MPB.

Here, we have studied the domain structures and octahedral tiltings of NBT- $x\%$ BT for  $x = 0, 4.5,$  and  $5.5$  by transmission electron microscopy (TEM) methods of bright field (BF) imaging and selected area electron diffraction (SAED). We found with increasing  $x$  that: (i) the size of polar

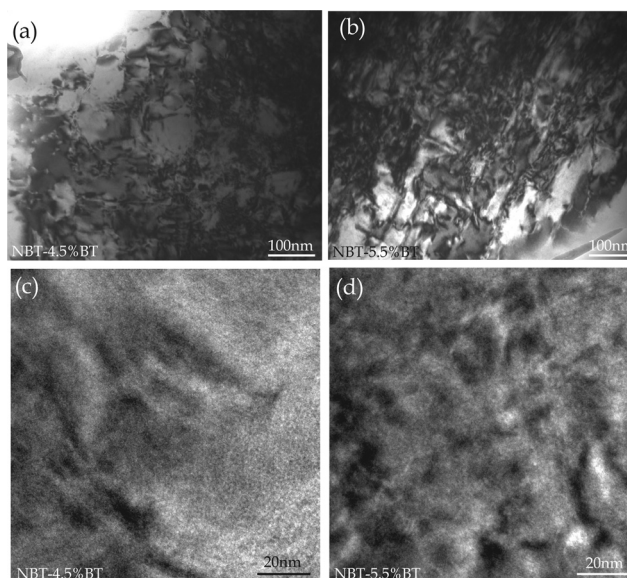


FIG. 1. TEM bright field images of (a) NBT-4.5%BT and (b) NBT-5.5%BT, which reveal enhanced density of polar nano-regions for NBT-5.5%BT than NBT-4.5%BT. High resolution image of polar nano-regions of (c) NBT-4.5%BT and (d) NBT-5.5%BT.

<sup>a)</sup>Electronic mail: jjyao@vt.edu.

nano-regions was refined, and their density increased; and (ii) the intensity of the octahedral in-phase  $1/2(0oe)$  tilting reflections in both  $[100]$  and  $[11\bar{2}]$  SAED patterns increased, revealing that the volume fraction of a  $T$  phase increases. These findings support that the mechanism of enhanced piezoelectricity near the MPB in NBT-BT is due not only to polarization rotations but also to polarization extension.

Single crystals of NBT- $x\%$ BT were grown by a self-flux technique.<sup>4</sup> Samples for TEM were prepared by mechanical polishing, followed by a dimple grinder thinning process, and finally by argon ion thinning. Electron diffraction and BF imaging were performed using a Philips EM 420 electron microscope working at 120 kV, with a double-tilt sample holder to enable access to the various zone axes.

Figures 1(a) and 1(b) show BF images for NBT-4.5%BT and NBT-5.5%BT. Polar nano-regions (PNR) are evident, similar to those previously reported by piezoforce microscopy (PFM).<sup>15</sup> The average size of these polar nano-regions was about 20–50 nm. The size of the nano-regions for NBT-5.5%BT was smaller than that for NBT-4.5%BT. Previous TEM studies of NBT have shown polar nano-regions of size around 50–100 nm.<sup>16</sup> Comparison of these prior results of NBT with the present ones (Figs. 1(a) and 1(b)) for  $x = 4.5$  and 5.5 will show that the PNR size is reduced with increasing  $x$ . This reduction in PNR size is more clearly shown in the higher resolution images given in Figs. 1(c) and 1(d), respectively. For  $x = 5.5$ , the ensemble of polar nano-regions had a notably higher degree of self-organization, consistent with prior PFM studies.<sup>15</sup> Such self-organization indicates that the system is able to relax its elastic energy by geometrically arranging the PNRs into improper ferroelastic domain bands.<sup>17</sup> Please note that this MPB boundary region ( $5.5 < x < 6.5$ ) is where the dielectric

and piezoelectric constants have been reported to be maximum.<sup>4,5</sup> Stress accommodated finer PNRs would result in a polydomain structure, which is more susceptible to electric field  $E$ . This could be manifested by changes in the PNR distribution as in an adaptive phase<sup>9</sup> or by induced local phase transformations confined to regions of high twin density.<sup>18</sup>

Electron diffraction patterns for NBT taken along different zone axes are shown in Figs. 2(a)–2(c). For NBT- $x$ at. %BT, the superlattice reflections are believed to originate from  $1/2(0oo)$  anti-phase and  $1/2(0oe)$  in-phase oxygen octahedral tiltings (where  $o$  designates odd values of the Miller indices, and  $e$  even) of limited spatial correlation,<sup>20–25</sup> which can be used to identify local  $R$  and  $T$  phase regions. For pure NBT, no obvious  $1/2(0oe)$  superlattice reflections were found in the SAED patterns (Fig. 2(a)), consistent with prior work.<sup>16</sup> This indicates limited to no tendency for short-range ordered in-phase oxygen octahedral tilted regions. One can thus infer very small to no volume fraction of  $T$  regions on the nanoscale.<sup>21,22,26</sup> However, along the  $[110]$  zone,  $1/2(0oo)$  superlattice reflections were notable, as marked by rings in the SAED pattern of Fig. 2(b). Figure 2(c) taken along the  $[11\bar{2}]$  zone, where both  $1/2(0oe)$  and  $1/2(0oo)$  reflections could be present, shows strong  $1/2(0oo)$  reflections (as marked by rings), but no  $1/2(0oe)$  ones. One can thus infer a high volume fraction ( $V_f$ ) of anti-phase tilted regions with  $R$  symmetry, with little to no  $V_f$  of in-phase tilted ones with  $T$  symmetry. Please note that previous studies have shown that the  $1/2(0oe)$  reflections of NBT become more intense in the range of 400–500 °C, where a  $T$  ferroelastic paraelectric phase exists.<sup>19</sup>

Next, we show the effect of BT content on the  $1/2(0oe)$  and  $1/2(0oo)$  reflections. Figures 2(d)–2(f) and 2(g)–2(i) show SAED patterns for  $x = 4.5$  and 5.5 taken along  $[001]$ ,  $[110]$ , and  $[11\bar{2}]$  zones, respectively. Relative to NBT, the intensity

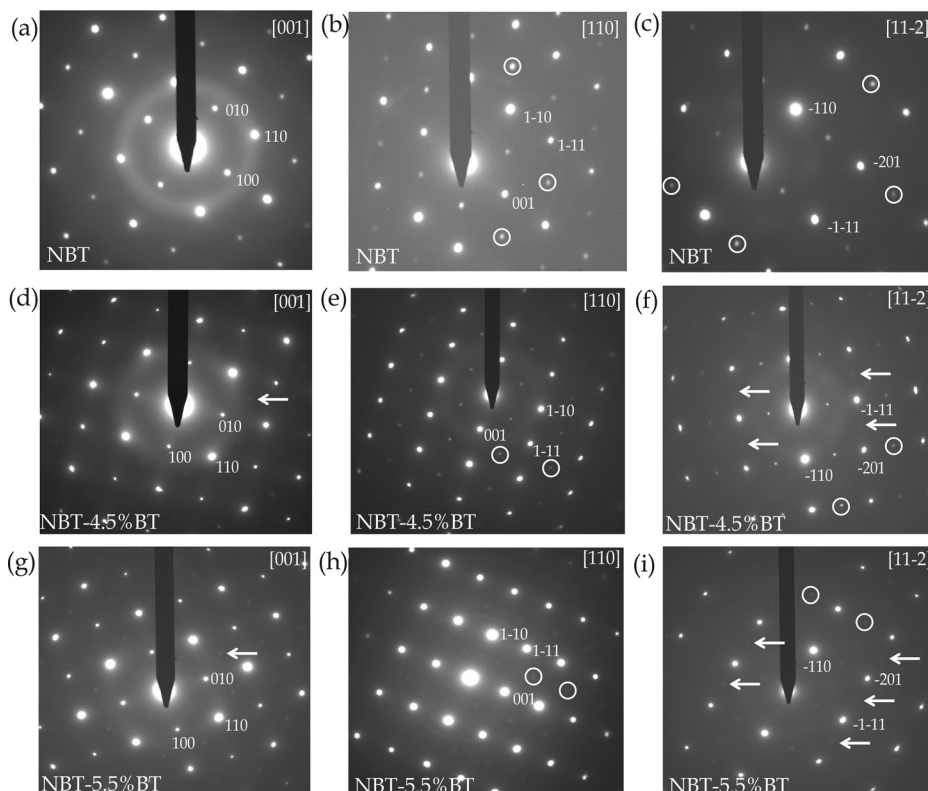


FIG. 2. SAED patterns for NBT (a)–(c) taken along  $[001]$ ,  $[110]$ ,  $[11\bar{2}]$  zone axis, respectively; NBT-4.5%BT (d)–(f); NBT-5.5%BT (g)–(i), where  $1/2(0oo)$  superlattice reflections are marked by rings,  $1/2(0oe)$  ones by arrows.

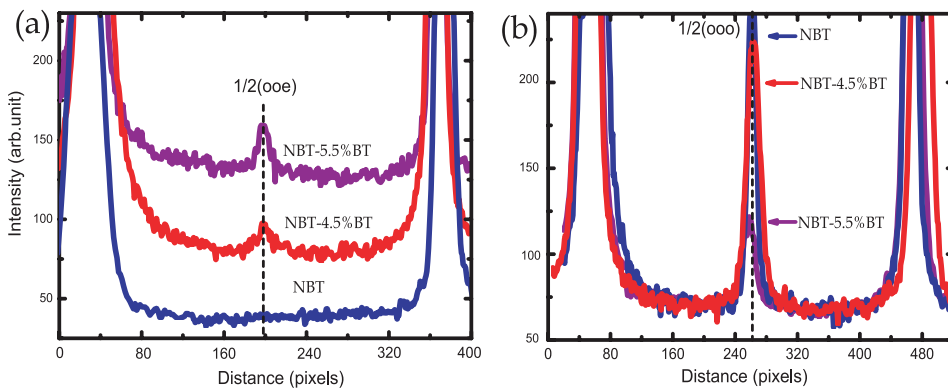


FIG. 3. (Color online) (a) and (b) show the illustration of line profiles of intensity for  $1/2(00e)$  and  $1/2(00o)$  reflections for the three compositions, in order to guide the eyes, line profiles of NBT-4.5%BT and NBT-5.5%BT in (g) have move upwards.

of the  $1/2(00e)$  reflections for NBT-4.5%BT can be seen to be increased (marked by arrows in Fig. 2(d)), whereas that of  $1/2(00o)$  was decreased (marked by rings in Fig. 2(e)). Furthermore, along the  $[11\bar{2}]$  zone, coexisting weak  $1/2(00e)$  and  $1/2(00o)$  reflections were found (as marked by arrows and rings, respectively in Fig. 2(f)). These observations demonstrate that the  $V_f$  of short-range ordered in-phase tilted regions is increased with  $x\%$ , and that of anti-phase tilted ones decreased. Regions of  $R$  and  $T$  symmetries on the nano-scale level coexist. Changes in the intensity of the  $1/2(00o)$  and  $1/2(00e)$  reflections continued with increasing BT content to  $x = 5.5$ : as can be seen in Figs. 2(g)–2(i) taken along the  $[001]$ ,  $[110]$ , and  $[11\bar{2}]$  zones, respectively. In this case, the intensity of the two superlattice reflections were nearly equal, indicating that the volume fraction of short-range ordered anti-phase tilted regions are the same.

In order to get more detailed information about the  $1/2(00o)$  and  $1/2(00e)$  reflections, one sketch of the peak intensities based on diffraction patterns is shown in Figs. 3(a) and 3(b). In this figure, it can be seen that the intensity of the  $1/2(00e)$  reflection is nearly zero for NBT and increases with increasing BT content. Furthermore, for the  $1/2(00o)$  reflection, the intensity decreased with increasing  $xat. \%BT$ . These data could infer that the  $V_f$  of short-range ordered in-phase tilted regions increased and that of anti-phase tilted regions decreased as the MPB is approached. Please note that this increased  $V_f$  of in-phase tilted regions within the average  $R$  phase is coincidental with a significant increase of  $d_{33}$  with  $xat. \%BT$  as the MPB is approached.<sup>3–5</sup>

The question now needs to be asked about why the increased density of local tetragonal distorted regions might be beneficial to the enhancement of the piezoelectric properties for NBT- $xat. \%BT$ . It has been reported that an electric field induced phase transition results in a giant strain for compositions near the MPB. The transition was initially ascribed to one between ferroelectric and antiferroelectric states under  $E$ ,<sup>27–29</sup> which remains controversial following Raman studies.<sup>30</sup> Soon thereafter, a field-induced transition between non-polar and ferroelectric phases was proposed,<sup>12–14</sup> where the nonpolar phase has a  $T$  structure.<sup>12</sup> We note that the increased density of local tetragonally distorted regions could contribute significantly to the total strain during an induced transition from non-polar to ferroelectric phases under  $E$ .

Recently, Damjanovic proposed that in addition to polarization rotation that polarization extension could result in enhanced electro-mechanical properties.<sup>31,32</sup> He suggested

that the presence of a long-range  $M$  phase may not by itself guarantee enhanced piezoelectricity, but rather structural instabilities having both polarization rotation and extension contributions could be more important near the MPB.<sup>31</sup> With regards to NBT- $x\%BT$ , our findings of enhanced local  $T$  distortions (or short-range ordered in-phase oxygen octahedral tilts) within the  $R$  phase on approaching the MPB supports the possibility that polarization extension makes significant contributions to the total piezoelectric response. The increasing  $T$  volume fraction within the  $R$  phase on approaching the MPB would result in enhanced electrically-induced macro-strains, via polarization extension. Furthermore, with increasing temperature between 25 °C and 130 °C, the electrically induced strain of NBT- $x\%BT$  is increased:<sup>33</sup> this could be the result of polarization extension, due to a temperature-driven phase transition.

In summary, we have studied the domain structure and octahedral tilting of NBT- $x\%BT$  for  $x = 0, 4.5$ , and  $5.5$  by TEM. We find with increasing  $x$ : (i) a refined size of polar nano-regions and an enhanced self-organization, and (ii) an increased intensity of the octahedral in-phase tilt  $1/2(00e)$  reflections and a decrease in the anti-phase  $1/2(00o)$  ones. This reveals that the volume fraction of the  $T$  phase increases with increasing  $x$  as the MPB is approached. The findings support that the mechanism of enhanced piezoelectricity for NBT- $x\%BT$  near the MPB has both polarization rotation and polarization extension contributions.

This work was financially supported by the National Science Foundation (Materials World Network) DMR-0806592, by the Department of Energy under DE-FG02-07ER46480, by the National Science Foundation of China 50602047, and by the Shanghai Municipal Government 08JC1420500. J. Yao also would like to thank the financial support from the China Scholarship Council. Authors also thank Dr. Z. K. Xu for useful discussion and the Nanoscale Characterization and Fabrication Laboratory in Virginia Tech for the instrumentation support and training.

<sup>1</sup>G. H. Haertling, *J. Am. Ceram. Soc.* **82**, 797 (1999).

<sup>2</sup>T. Takenaka, K. Maruyama, and K. Sakata, *Jpn. J. Appl. Phys.* **30**, 2236 (1991).

<sup>3</sup>Y. M. Chiang, G. W. Farrey, and A. N. Soukhojak, *Appl. Phys. Lett.* **73**, 3683 (1998).

<sup>4</sup>Q. Zhang, Y. Zhang, F. Wang, Y. Wang, D. Lin, X. Zhao, H. Luo, W. Ge, and D. Viehland, *Appl. Phys. Lett.* **95**, 102904 (2009).

<sup>5</sup>Y. P. Guo, M. Y. Gu, H. S. Luo, Y. Liu, and R. L. Withers, *Phys. Rev. B* **83**, 054118 (2011).

- <sup>6</sup>F. Cordero, F. Craciun, F. Trequattrini, E. Mercadelli, and C. Galassi, *Phys. Rev. B* **81**, 144124 (2010).
- <sup>7</sup>W. Jo, J. E. Daniels, J. L. Jones, X. L. Tan, P. A. Thomas, D. Damjanovic, and J. Rödel, *J. Appl. Phys.* **109**, 014110 (2011).
- <sup>8</sup>B. Noheda, D. E. Cox, G. Shirane, J. A. Gonzalo, L. E. Cross, and S.-E. Park, *Appl. Phys. Lett.* **74**, 2059 (1999).
- <sup>9</sup>D. Viehland, *J. Appl. Phys.* **88**, 4794 (2000).
- <sup>10</sup>E. Aksel, J. S. Forrester, J. L. Jones, P. A. Thomas, K. Page, and M. R. Suchomel, *Appl. Phys. Lett.* **98**, 152901 (2011).
- <sup>11</sup>S. Gorfman and P. A. Thomas, *J. Appl. Crystallogr.* **43**, 1409 (2010).
- <sup>12</sup>M. Hinterstein, M. Knapp, M. Holzel, W. Jo, A. Cervellino, H. Ehrenberg, and H. Fuess, *J. Appl. Crystallogr.* **43**, 1314 (2010).
- <sup>13</sup>J. Kling, X. L. Tan, W. Jo, H.-J. Kleebe, H. Fuess, and J. Rödel, *J. Am. Ceram. Soc.* **93**, 2452 (2010).
- <sup>14</sup>J. Daniels, W. Jo, J. Rödel, and J. Jones, *Appl. Phys. Lett.* **95**, 032904 (2009).
- <sup>15</sup>J. J. Yao, L. Yan, W. W. Ge, L. Luo, J. F. Li, D. Viehland, Q. H. Zhang, and H. Luo, *Phys. Rev. B* **83**, 054107 (2011).
- <sup>16</sup>J. J. Yao, W. W. Ge, Y. D. Yang, L. Luo, J. F. Li, D. Viehland, S. Bhattacharyya, Q. H. Zhang, and H. S. Luo, *J. Appl. Phys.* **108**, 064114 (2010).
- <sup>17</sup>F. M. Bai, J. F. Li, and D. Viehland, *Appl. Phys. Lett.* **85**, 2313 (2004).
- <sup>18</sup>W. W. Cao and C. A. Randall, *J. Phys. Chem. Solids* **57**, 1499 (1996).
- <sup>19</sup>J. J. Yao, W. W. Ge, L. Luo, J. F. Li, D. Viehland, and H. Luo, *Appl. Phys. Lett.* **96**, 222905 (2010).
- <sup>20</sup>G. Jones and P. Thomas, *Acta Crystallogr. B* **58**, 168 (2002).
- <sup>21</sup>C. W. Tai and Y. Lereah, *Appl. Phys. Lett.* **95**, 062901 (2009).
- <sup>22</sup>V. Dorcet and G. Trolliard, *Acta Mater.* **56**, 1753 (2008).
- <sup>23</sup>C. Ma, X. Tan, E. Dul'kin, and M. J. Roth, *J. Appl. Phys.* **108**, 104105 (2010).
- <sup>24</sup>L. A. Schmitt, M. Hinterstein, and H.-J. Kleebe, *J. Appl. Crystallogr.* **43**, 805 (2010).
- <sup>25</sup>L. A. Schmitt, J. Kling, M. Hinterstein, M. Hoelzel, W. Jo, H.-J. Kleebe, and H. Fuess, *J. Mater. Sci.* **46**, 4368 (2011).
- <sup>26</sup>J. J. Yao, Y. D. Yang, N. Monsegue, Y. X. Li, J. F. Li, Q. H. Zhang, W. W. Ge, H. S. Luo, and D. Viehland, *Appl. Phys. Lett.* **98**, 132903 (2011).
- <sup>27</sup>S. T. Zhang, A. B. Kounga, E. Aulbach, H. Ehrenberg, and J. Rödel, *Appl. Phys. Lett.* **91**, 112906 (2007).
- <sup>28</sup>S. T. Zhang, A. B. Kounga, E. Aulbach, W. Jo, T. Granzow, H. Ehrenberg, and J. Rödel, *J. Appl. Phys.* **103**, 034108 (2008).
- <sup>29</sup>W. Jo, T. Granzow, E. Aulbach, J. Rödel, and D. Damjanovic, *J. Appl. Phys.* **105**, 094102 (2009).
- <sup>30</sup>B. Wylie-Van Eerd, D. Damjanovic, N. Klein, N. Setter, and J. Trodahl, *Phys. Rev. B* **82**, 104112 (2010).
- <sup>31</sup>D. Damjanovic, *IEEE Trans. Ultrason. Ferroelectr. Freq. Control* **56**, 1574 (2009).
- <sup>32</sup>D. Damjanovic, *Appl. Phys. Lett.* **97**, 062906 (2010).
- <sup>33</sup>W. W. Ge, Q. H. Zhang, Z. G. Wang, J. J. Yao, J. F. Li, H. S. Luo, and D. Viehland, *Phys. Status Solidi (RRL)* **5**, 356 (2011).